

Critical current density of a spin-torque oscillator with an in-plane magnetized free layer and an out-of-plane magnetized polarizer

R. Matsumoto¹ and H. Imamura^{1, a)}

¹*National Institute of Advanced Industrial Science and Technology (AIST),
Spintronics Research Center, Tsukuba, Ibaraki 305-8568,
Japan*

(Dated: 10 March 2022)

Spin-torque induced magnetization dynamics in a spin-torque oscillator with an in-plane (IP) magnetized free layer and an out-of-plane (OP) magnetized polarizer under IP shape-anisotropy field (H_k) and applied IP magnetic field (H_a) was theoretically studied based on the macrospin model. The rigorous analytical expression of the critical current density (J_{c1}) for the OP precession was obtained. The obtained expression successfully reproduces the experimentally obtained H_a -dependence of J_{c1} reported in [D. Houssameddine *et al.*, Nat. Mater. 6, 447 (2007)].

PACS numbers: 75.78.-n, 85.75.-d, 85.70.Kh, 72.25.-b

Keywords: Spin-torque oscillator

^{a)}Electronic mail: h-imamura@aist.go.jp

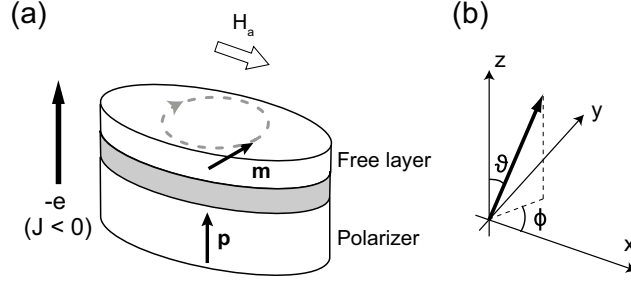


FIG. 1. (a) Spin-torque oscillator consisting of in-plane (IP) magnetized free layer and out-of-plane (OP) magnetized polarizer layer. IP magnetic field (H_a) is applied parallel to easy axis of the free layer. Negative current density ($J < 0$) is defined as electrons flowing from the polarizer layer to the free layer. The unit vector \mathbf{m} represents the direction of magnetization in the free layer. (b) Definitions of Cartesian coordinates (x, y, z), polar angle (θ) and azimuthal angle (ϕ).

A spin-torque oscillator (STO)¹⁻⁶ with an in-plane (IP) magnetized free layer and an out-of-plane (OP) magnetized polarizer⁷⁻¹⁵ has been attracting a great deal of attention as microwave field generators^{12,16-20} and high-speed field sensors²¹⁻²⁶. The schematic of the STO is illustrated in Fig. 1(a). When the current density (J) of the applied dc current exceeds the critical value (J_{c1}), the 360° in-plane precession of the free layer magnetization, so-called OP precession, is induced by the spin torque. Thanks to the OP precession, a large-amplitude microwave field can be generated,^{12,14,15} and a high microwave power can be obtained through the additional analyzer.⁸

The critical current density, J_{c1} , for the OP precession of this type of STO has been extensively studied both experimentally^{8,15} and theoretically.^{7,9-11,13,27} In 2007, D. Houssameddine *et al.* experimentally found that J_{c1} was approximately expressed as $J_{c1} \propto H_k + 2H_a$ where H_k is IP shape-anisotropy field and H_a is the applied IP magnetic field. In theoretical studies, the effect of H_k and H_a on J_{c1} has been studied analytically and numerically. U. Ebels *et al.* proposed an approximate expression of J_{c1} , however, as we shall show later, it gives exact solution only in the limit of $H_a = 0$ and $H_k \rightarrow 0$. Lacoste *et al.* obtained the lower current boundary for the existence of OP precession¹³ which gives some insights into J_{c1} , however, it could be lower than J_{c1} . To our best knowledge, J_{c1} of this type of STO is still controversial and a systematic understanding of J_{c1} in the presence of H_k and H_a is necessary.

In this letter, we theoretically analyzed spin-torque induced magnetization dynamics in

the STO with an IP magnetized free layer and an OP magnetized polarizer in the presence of H_k and H_a based on the macrospin model. We obtained the rigorous analytical expression of J_{c1} and showed that it successfully reproduces the experimentally obtained H_a -dependence of the critical current reported by D. Houssameddine *et al.*⁸

The system we consider is schematically illustrated in Figs. 1(a) and (b). The shape of the free layer is either a circular cylinder or an elliptic cylinder. The lateral size of the nanopillar is assumed to be so small that the magnetization dynamics can be described by the macrospin model. Directions of the magnetization in the free layer and in the polarizer are represented by the unit vectors \mathbf{m} and \mathbf{p} , respectively. The vector \mathbf{p} is fixed to the positive z -direction. The negative current is defined as electrons flowing from the polarizer to the free layer. The applied IP magnetic field, H_a , is assumed to be parallel to the magnetization easy axis of the free layer. The easy axis is parallel to x -axis.

The energy density of the free layer is given by²⁸

$$E = \frac{1}{2}\mu_0 M_s^2 (N_x m_x^2 + N_y m_y^2 + N_z m_z^2) + K_{u1} \sin^2 \theta - \mu_0 M_s H_a \sin \theta \cos \phi. \quad (1)$$

Here $(m_x, m_y, m_z) = (\sin \theta \cos \phi, \sin \theta \sin \phi, \cos \theta)$, and θ and ϕ are the polar and azimuthal angles of \mathbf{m} as shown in Fig. 1(b). The demagnetization coefficients, N_x , N_y , and N_z are assumed to satisfy $N_z \gg N_y \geq N_x$. K_{u1} is the first-order crystalline anisotropy constant, μ_0 is the vacuum permeability, M_s is the saturation magnetization of the free layer, and H_a is applied IP magnetic field.

Hereafter we conduct the analysis with dimensionless expressions. The dimensionless energy density of the free layer is given by

$$\epsilon = \frac{1}{2}(N_x m_x^2 + N_y m_y^2 + N_z m_z^2) + k_{u1} \sin^2 \theta - h_a \sin \theta \cos \phi. \quad (2)$$

Here, k_{u1} and h_a are defined as $k_{u1} = K_{u1}/(\mu_0 M_s^2)$ and $h_a = H_a/M_s$. We discuss on the spin-torque induced magnetization dynamics at $h_a \geq 0$ in this letter, however, the dynamics at $h_a < 0$ can be calculated in the similar way.

The spin-torque induced dynamics of \mathbf{m} in the presence of applied current is described

by the following Landau-Lifshitz-Gilbert equation,²⁸

$$(1 + \alpha^2) \frac{d\theta}{d\tau} = h_\phi + \chi \sin \theta + \alpha h_\theta, \quad (3)$$

$$(1 + \alpha^2) \sin \theta \frac{d\phi}{d\tau} = -h_\theta + \alpha(h_\phi + \chi \sin \theta), \quad (4)$$

where τ , χ , h_θ , and h_ϕ are the dimensionless quantities representing time, spin torque, and θ , ϕ components of effective magnetic field, \mathbf{h}_{eff} , respectively. \mathbf{h}_{eff} is given by $\mathbf{h}_{\text{eff}} = -\nabla\epsilon$. α is the Gilbert damping constant. The dimensionless time is defined as $\tau = \gamma_0 M_s t$, where $\gamma_0 = 2.21 \times 10^5$ m/(A·s) is the gyromagnetic ratio and t is the time. h_θ and h_ϕ are given by

$$h_\theta = \cos \theta \left[2 \sin \theta \left(\frac{h_k}{2} \cos^2 \phi - k_{\text{ul}}^{\text{eff}} \right) + h_a \cos \phi \right], \quad (5)$$

$$h_\phi = -\frac{h_k}{2} \sin \theta \sin 2\phi - h_a \sin \phi. \quad (6)$$

Here h_k is dimensionless IP shape-anisotropy field being expressed as $h_k = N_y - N_x = H_k/M_s$. $k_{\text{ul}}^{\text{eff}}$ is defined as $k_{\text{ul}}^{\text{eff}} = K_{\text{ul}}^{\text{eff}}/(\mu_0 M_s^2) = k_{\text{ul}} - (N_z - N_y)/2$. $K_{\text{ul}}^{\text{eff}}$ is the effective first-order anisotropy constant where the demagnetization energy is subtracted. Since we are interested in the spin-torque induced magnetization dynamics of the IP magnetized free layer, we concentrate on $k_{\text{ul}}^{\text{eff}} < 0$. The prefactor of the spin-torque term, χ , is expressed as

$$\chi = \eta(\theta) \frac{\hbar}{2e} \frac{J}{\mu_0 M_s^2 d}, \quad (7)$$

where $\eta(\theta) = P/(1 + P^2 \cos \theta)$ is spin-torque efficiency, P is the spin polarization, J is the applied current density, d is the thickness of the free layer, e (> 0) is the elementary charge and \hbar is the Dirac constant. For convenience of discussion, the sign of Eq. (7) is taken to be opposite to that in Ref. 28.

In the absence of the current, i.e., $J = 0$, the angles of the equilibrium direction of \mathbf{m} are obtained as $\theta_{\text{eq}} = \pi/2$ and $\phi_{\text{eq}} = 0$ by minimizing ϵ with respect to θ and ϕ . Application of J changes θ and ϕ from its equilibrium values. If the magnitude of J is smaller than the critical value, the magnetization converges to a certain fixed point.²⁹ The equations determining the polar and azimuthal angles of the fixed point (θ_0, ϕ_0) are obtained by setting $d\theta/d\tau = 0$ and $d\phi/d\tau = 0$ as

$$h_\theta^0 = 0, \quad (8)$$

$$h_\phi^0 = -\chi \sin \theta_0. \quad (9)$$

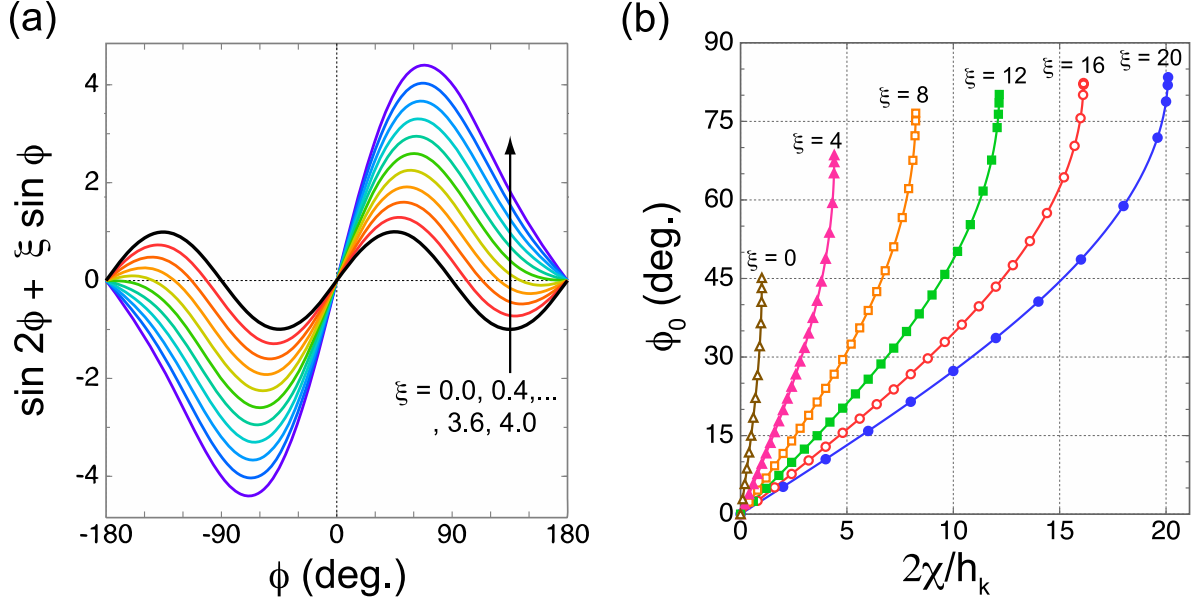


FIG. 2. (a) Function, $\sin 2\phi + \xi \sin \phi$, is plotted as against ϕ . Value of ξ is varied from 0.0 to 4.0. (b) Spin-torque magnitude (χ) dependence of ϕ at fixed point (ϕ_0) in the presence of IP shape anisotropy field. χ is defined in Eq. (7), and it is proportional to J . Curves represent the analytical results obtained by Eq. (10). Open or solid circles, squares, and triangles represent numerical calculation results.

The fixed point around the equilibrium direction ($\theta_{\text{eq}} = \pi/2$, $\phi_{\text{eq}}=0$) are obtained as follows. Assuming $|\phi_0| \leq \pi/2$, i.e., $\cos \phi_0 \geq 0$ and noting $k_{\text{ul}}^{\text{eff}} < 0$, one can see that the quantity in the square bracket of Eq. (5) is positive and $\theta_0 = \pi/2$ to satisfy $h_\theta^0 = 0$. Substituting $\theta_0 = \pi/2$ to $h_\phi^0 = -\chi \sin \theta_0$, the equation determining ϕ_0 is obtained as

$$\sin 2\phi_0 + \xi \sin \phi_0 = 2\chi/h_k, \quad (10)$$

where $\xi = 2h_a/h_k$. Since Eq. (10) does not contain the Gilbert damping constant, α , ϕ_0 is independent of α . In Fig. 2(a), the function, $\sin 2\phi + \xi \sin \phi$, is plotted against ϕ for various values of $0 \leq \xi \leq 4$. One can clearly see that the azimuthal angle of the maximum (minimum) increases (decreases) towards $\pi/2$ ($-\pi/2$) with increase of ξ . The azimuthal angle of the fixed point is given by the intersection of this sinusoidal curve and a horizontal line at $2\chi/h_k$, and it increases with increase of $2\chi/h_k$ as shown in Fig. 2(b). In Fig. 2(b), the curves represent the analytical results obtained by Eq. (10) and the symbols represent the numerical results obtained by directly solving the Eqs. (3) and (4) with $\alpha = 0.02$, $h_k = 0.01$, and $k_{\text{u}}^{\text{eff}} = -0.4$. The analytical and simulation results agree very well with each other. We

also performed numerical simulations for wide range of α and confirmed that the numerical results of ϕ_0 are independent of α as predicted by the analytical results. In the numerical simulations, the current density was gradually increased from zero. At each current density, the simulation was run long enough for the polar and azimuthal angles to be converged to θ_0 and ϕ_0 .

Numerical simulations showed that there exists a critical current density, J_{c1} , above which the OP precession is induced. For $J > 0$, J_{c1} is obtained by calculating the maximum value (Λ) of the left hand side (LHS) of Eq. (10). If $2\chi/h_k$ is larger than Λ , there is no fixed point and the limit cycle corresponding to the OP precession is induced. Hereafter we consider the case of $J > 0$, however, the critical current density for $J < 0$ can be obtained in the similar way by calculating the minimum value.

At the maximum, the derivative of the LHS of Eq. (10) with respect to ϕ_0 is zero, that is,

$$2 \cos 2\phi_0 + \xi \cos \phi_0 = 0. \quad (11)$$

Expressing cosine functions by $\tan \phi_0$, one can easily obtain the solution of Eq. (11) as

$$\phi_{c1} = \arctan \left[\frac{1}{2\sqrt{2}} \sqrt{\xi^2 + 8 + \xi \sqrt{\xi^2 + 32}} \right], \quad (12)$$

where the subscript ‘‘c1’’ stands for the critical value corresponding to J_{c1} . Fig. 3(a) shows ξ dependence of ϕ_{c1} given by Eq. (12). $\phi_{c1} = \pi/4$ for $\xi = 0$, i.e., $h_a = 0$. It monotonically increases with increase of ξ and reaches $\pi/2$ in the limit of $\xi \rightarrow \infty$, i.e., $h_k \rightarrow 0$.

The maximum value, Λ , can be obtained by substituting $\phi = \phi_{c1}$ into the LHS of Eq. (10) as

$$\Lambda = \frac{\sqrt{X+8} (\xi \sqrt{X+16} + 4\sqrt{2})}{X+16}, \quad (13)$$

where $X = \xi(\xi + \sqrt{\xi^2 + 32})$. Equating this maximum value with $2\chi/h_k$ and using Eq. (7), the critical current density is obtained as

$$J_{c1} = \frac{e\mu_0 M_s d H_k}{\hbar P} \frac{\sqrt{X+8} (\xi \sqrt{X+16} + 4\sqrt{2})}{X+16}. \quad (14)$$

This is the main result of this letter. It should be noted J_{c1} is also independent of α . In the absence of the applied IP magnetic field, i.e., $H_a = 0$, Eq. (14) becomes

$$J_{c1}|_{H_a=0} = \frac{e\mu_0 M_s d H_k}{\hbar P}. \quad (15)$$

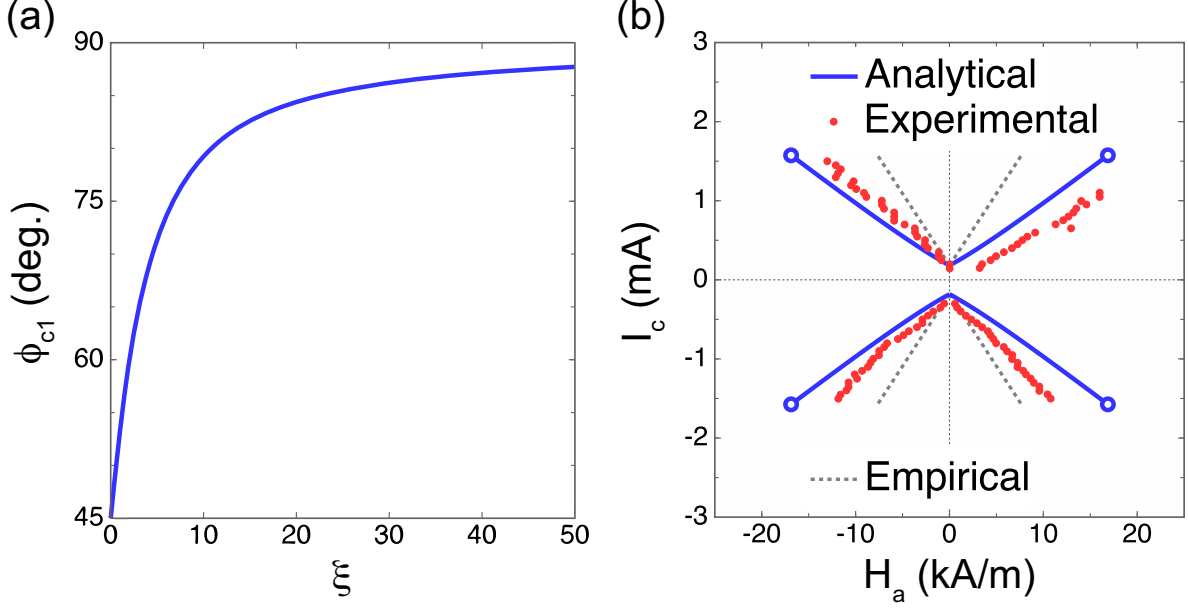


FIG. 3. (a) Analytically-calculated ξ dependence of critical ϕ (ϕ_{c1}). ξ is ratio between H_a and IP shape anisotropy field (H_a), being $\xi = 2H_a/H_k$. (b) H_a dependence of critical current (I_c) for OP precession. Solid blue curves represent plots of analytical expression (Eq. (14)). H_k of 4 kA/m is assumed. Open blue circles represent critical current above which the OP precession can not be maintained. Red dots represent past experimental results (redrawn from Ref. 8). Dotted gray lines represent the empirically approximated value proposed in Ref. 8.

In the limit of $H_k \rightarrow 0$, it reduces to

$$\lim_{H_k \rightarrow 0} J_{c1} = \frac{2e\mu_0 M_s d H_a}{\hbar P}. \quad (16)$$

For small magnetic field such that $H_a \ll H_k$, i.e., $\xi \ll 1$, it can be approximated as

$$J_{c1} \simeq \frac{e\mu_0 M_s d}{\hbar P} \left(H_k + \sqrt{2} H_a \right), \quad (17)$$

by noting that the Taylor expansion of Λ around $\xi = 0$ is given by $\Lambda = 1 + \xi/\sqrt{2} + \xi^2/16 + O(\xi^3)$.

Once the current density, J , exceeds J_{c1} , the OP precession is excited and further increase of J moves the trajectory towards the south pole ($\theta = \pi$). Around $\theta = 0$ and π , there exist the fixed points other than $\theta_0 = \pi/2$, which are determined by

$$2 \sin \theta_0 \left(\frac{h_k}{2} \cos^2 \phi_0 - k_{ul}^{\text{eff}} \right) + h_a \cos \phi_0 = 0, \quad (18)$$

$$\frac{h_k}{2} \sin \theta_0 \sin 2\phi_0 + h_a \sin \phi_0 = \chi \sin \theta_0. \quad (19)$$

After some algebra, the fixed point is obtained as

$$\theta_0 = \arcsin \left(\frac{h_a \sqrt{(k_{u1}^{\text{eff}})^2 + \chi^2}}{2 \left[(k_{u1}^{\text{eff}})^2 + \chi^2 \right] - h_k k_{u1}^{\text{eff}}} \right), \quad (20)$$

$$\phi_0 = -\arctan \frac{\chi}{k_{u1}^{\text{eff}}}, \quad (21)$$

where $\pi/2 < |\phi_0| \leq \pi$. In the absence of the applied IP magnetic field, i.e., $h_a = 0$, the polar angle of the fixed point is $\theta_0 = 0$ or π . It is difficult to obtain the exact analytical expression for the critical current density, J_{c2} , above which the OP precession can not be maintained, and \mathbf{m} stays at the fixed point given by Eqs. (20) and (21). Since the average polar angle of the trajectory of the OP precession is determined by the competition between the damping torque and spin torque, this critical current density should depend on α . The approximate expression was obtained by Ebels *et al.*¹¹ as

$$J_{c2} \simeq -\frac{4\alpha ed K_{u1}^{\text{eff}}}{\hbar P}, \quad (22)$$

which agrees well with the macrospin simulation results.

Let us compare our results with the experimental results reported by D. Houssameddine *et al.*⁸ Figure 3(b) shows the applied IP magnetic field, H_a , dependence of critical current (I_c) for the OP precession. The analytical results of Eq. (14) are plotted by the solid (blue) line and the experimental results are plotted by the (red) dots. The critical current corresponding to J_{c2} are also shown by open (blue) circles. In the analytical calculation, the following parameters indicated in Ref. 8 are assumed: $\alpha = 0.02$, $M_s = 866$ kA/m, the junction area is $30 \times 35 \times \pi$ nm², $d = 3.5$ nm, $P = 0.3$, $H_k = 4$ kA/m. The dotted (gray) lines represent the approximated values proposed in Ref. 8, $I_c \propto H_k + 2H_a$. One can clearly see that the analytical results of Eq. (14) reproduces the experimental results very well. The agreement is much better than the approximated values of Ref. 8. As shown in Eq. (17), the critical current for small magnetic field can be approximated as $I_c \propto H_k + \sqrt{2}H_a$ rather than $I_c \propto H_k + 2H_a$.

In summary, we theoretically studied spin-torque induced magnetization dynamics in an STO with an IP magnetized free layer and an OP magnetized polarizer. We obtained the rigorous analytical expressions of J_{c1} for the OP precession in the presence of IP shape-anisotropy field (H_k) and applied IP magnetic field (H_a). The expression reproduces the

experimental results very well and revealed that the critical current is proportional to $H_k + \sqrt{2}H_a$ for $H_a \ll H_k$.

ACKNOWLEDGMENTS

This work was supported by JSPS KAKENHI Grant Number 16K17509.

REFERENCES

- ¹J. C. Slonczewski, *J. Magn. Magn. Mater.* **159**, L1 (1996).
- ²L. Berger, *Phys. Rev. B* **54**, 9353 (1996).
- ³M. Tsoi, A. G. M. Jansen, J. Bass, W.-C. Chiang, M. Seck, V. Tsoi, and P. Wyder, *Phys. Rev. Lett.* **80**, 4281 (1998).
- ⁴S. I. Kiselev, J. C. Sankey, I. N. Krivorotov, N. C. Emley, R. J. Schoelkopf, R. A. Buhrman, and D. C. Ralph, *Nature* **425**, 380 (2003).
- ⁵A. M. Deac, A. Fukushima, H. Kubota, H. Maehara, Y. Suzuki, S. Yuasa, Y. Nagamine, K. Tsunekawa, D. D. Djayaprawira, and N. Watanabe, *Nat. Phys.* **4**, 803 (2008).
- ⁶A. Slavin and V. Tiberkevich, *IEEE Transactions on Magnetics* **45**, 1875 (2009).
- ⁷K. J. Lee, O. Redon, and B. Dieny, *Appl. Phys. Lett.* **86**, 022505 (2005).
- ⁸D. Houssameddine, U. Ebels, B. Delaet, B. Rodmacq, I. Firastrau, F. Ponthenier, M. Brunet, C. Thirion, J.-P. Michel, L. Prejbeanu-Buda, M.-C. Cyrille, O. Redon, and B. Dieny, *Nat. Mater.* **6**, 447 (2007).
- ⁹I. Firastrau, U. Ebels, L. Buda-Prejbeanu, J. C. Toussaint, C. Thirion, and B. Dieny, *J. Magn. Magn. Mater.* **310**, 2029 (2007).
- ¹⁰T. J. Silva and M. W. Keller, *IEEE Trans. Magn.* **46**, 3555 (2010).
- ¹¹U. Ebels, D. Houssameddine, I. Firastrau, D. Gusakova, C. Thirion, B. Dieny, and L. D. Buda-Prejbeanu, *Phys. Rev. B* **78**, 024436 (2008).
- ¹²H. Suto, T. Yang, T. Nagasawa, K. Kudo, K. Mizushima, and R. Sato, *J. Appl. Phys.* **112**, 083907 (2012).
- ¹³B. Lacoste, L. D. Buda-Prejbeanu, U. Ebels, and B. Dieny, *Phys. Rev. B* **88**, 054425 (2013).

- ¹⁴S. Bosu, H. Sepehri-Amin, Y. Sakuraba, M. Hayashi, C. Abert, D. Suess, T. Schrefl, and K. Hono, *Appl. Phys. Lett.* **108**, 072403 (2016).
- ¹⁵R. Hiramatsu, H. Kubota, S. Tsunegi, S. Tamaru, K. Yakushiji, A. Fukushima, R. Matsumoto, H. Imamura, and S. Yuasa, *Appl. Phys. Express* **9**, 053006 (2016).
- ¹⁶X. Zhu and J. G. Zhu, *IEEE Trans. Magn.* **42**, 2670 (2006).
- ¹⁷J. G. Zhu, X. Zhu, and Y. Tang, *IEEE Trans. Magn.* **44**, 125 (2008).
- ¹⁸Y. Wang, Y. Tang, and J.-G. Zhu, *J. Appl. Phys.* **105**, 07B902 (2009).
- ¹⁹M. Igarashi, Y. Suzuki, H. Miyamoto, Y. Maruyama, and Y. Shiroishi, *IEEE Trans. Magn.* **45**, 3711 (2009).
- ²⁰K. Kudo, H. Suto, T. Nagasawa, K. Mizushima, and R. Sato, *Appl. Phys. Express* **8**, 103001 (2015).
- ²¹K. Kudo, T. Nagasawa, K. Mizushima, H. Suto, and R. Sato, *Appl. Phys. Express* **3**, 043002 (2010).
- ²²P. M. Braganca, B. A. Gurney, B. A. Wilson, J. A. Katine, S. Maat, and J. R. Childress, *Nanotechnology* **21**, 235202 (2010).
- ²³H. Suto, T. Nagasawa, K. Kudo, K. Mizushima, and R. Sato, *Appl. Phys. Express* **4**, 013003 (2011).
- ²⁴W. H. Rippard, A. M. Deac, M. R. Pufall, J. M. Shaw, M. W. Keller, S. E. Russek, G. E. W. Bauer, and C. Serpico, *Phys. Rev. B* **81**, 014426 (2010).
- ²⁵H. Kubota, K. Yakushiji, A. Fukushima, S. Tamaru, M. Konoto, T. Nozaki, S. Ishibashi, T. Saruya, S. Yuasa, T. Taniguchi, H. Arai, and H. Imamura, *Appl. Phys. Express* **6**, 103003 (2013).
- ²⁶H. Suto, T. Nagasawa, K. Kudo, K. Mizushima, and R. Sato, *Nanotechnology* **25**, 245501 (2014).
- ²⁷H. Morise and S. Nakamura, *Phys. Rev. B* **71**, 014439 (2005).
- ²⁸M. D. Stiles and J. Miltat, “Spin-transfer torque and dynamics,” in *Spin Dynamics in Confined Magnetic Structures III*, Topics in Applied Physics, Vol. 101, edited by B. Hillebrands and A. Thiaville (Springer Berlin Heidelberg, 2006) pp. 225–308.
- ²⁹G. Bertotti, I. D. Mayergoyz, and C. Serpico, in *Nonlinear Magnetization Dynamics in Nanosystems*, Elsevier Series in Electromagnetism (Elsevier, 2009) pp. 1–466.